Immersive Operation of a Semi-Autonomous Aerial Platform for Detecting and Mapping Radiation

P. Dayani, N. Orr, V. Saran, N. Hu, S. Krishnaswamy, A. Thomopoulos, E. Wang, J. Bae, E. Zhang, D. McPherson, J. Menke, A. Moran, B. Quiter, A. Yang, and K. Vetter

***Abstract*—Recent advancements in radiation detection and computer vision have enabled small unmanned aerial systems (sUASs) to produce 3D radiation maps, for example, composed of gamma-rays and neutrons, in real-time. Currently these state-of-the-art systems require two operators: one to pilot the sUAS and another operator to monitor the detected radiation. In this work we present a system that integrates real-time 3D radiation visualization with semi-autonomous sUAS control. Our Virtual Reality interface enables a single operator to define trajectories using waypoints to abstract complex flight control and utilize the semi-autonomous maneuvering capabilities of the sUAS. The interface also displays a fused radiation visualization and environment map, thereby enabling simultaneous remote operation and radiation monitoring by a single operator. This interface and its underlying framework serves as the basis for development of a single system that can deploy and autonomously control a fleet of radiation-mapping sUASs.**

I. Introduction

The ability to accurately detect and map radiological materials remains critical in nuclear security; nuclear emergency response; and the operation, decommissioning, and remediation of nuclear facilities. These applications require an effective visualization of radiation data to allow operators to assess complex scenes and to make informed decisions.

Radiation can now be effectively mapped by implementing 3D Scene Data Fusion (SDF) [1] that combines 3D radiation with environment data. The Localization and Mapping Platform (LAMP), a lightweight device that executes SDF, can be paired with gamma-ray and neutron detectors as well as gamma-ray imagers to generate radiation maps [2], [3]. LAMPs— referring to any variants including the Neutron Gamma LAMP (NG LAMP)— have already performed SDF on-board sUASs, leading to unprecedented capabilities [4] in locating radiological material and responding to its release. An sUAS can efficiently map environments with challenging terrain, dangerous conditions, or otherwise inaccessible areas.

Manuscript received June 21, 2021. Dayani, Orr, and Saran contributed equally. The project or effort depicted was or is sponsored by the Department of the Defense, Defense Threat Reduction Agency under contract HDTRA1-18-1-0027. The content of the information does not necessarily reflect the position or the policy of the federal government, and no official endorsement should be inferred. The project is also supported in part by a PCARI grant and an ONR grant N00014-19-1-2066.

P. Dayani, N. Orr, V. Saran, N. Hu, S. Krishnaswamy, A. Thomopoulos, E. Wang, J. Bae, E. Zhang, D. McPherson, J. Menke, and A. Yang are with the Department of Electrical Engineering and Computer Sciences and K. Vetter is with the Department of Nuclear Engineering, University of California, Berkeley, CA 94720 USA.

A. Moran, B. Quiter, and K. Vetter are with the Applied Nuclear Physics Program at Lawrence Berkeley National Laboratory, Berkeley, CA 94720 USA.

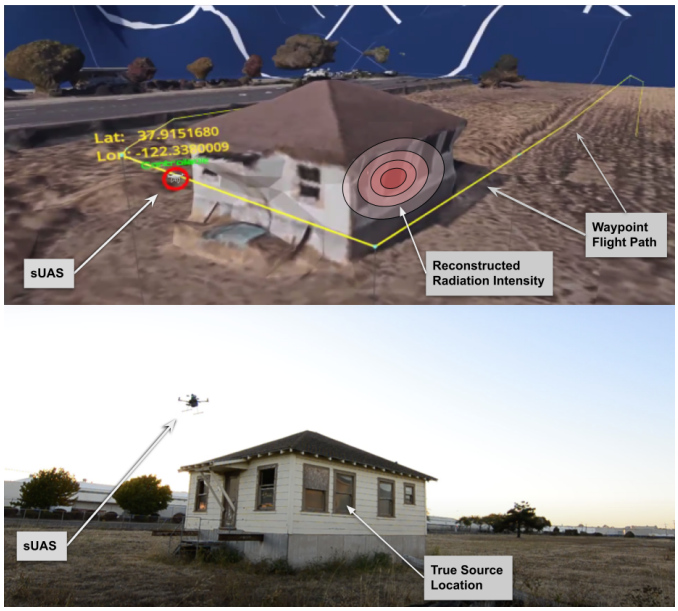

Fig. 1. Top: Conceptual illustration of a radiation mapping mission utilizing the new virtual reality interface. It allows an operator to command a radiation detector-equipped sUAS and to visualize radiation intensities reconstructed on 3D surfaces in real-time using the sUAS-mounted Localization and Mapping Platform. A 3D model of the sUAS (circled in red) and a baseline 3D satellite imagery map represent the real-world location (bottom) of the sUAS and its surroundings. The square building shown has a side length of about 8 meters. As the sUAS is directed on a waypoint-based flight by the operator from within this VR interface, detected radiation activity is overlaid on the baseline map. Isosurfaces of the reconstructed intensities are indicated here conceptually. These isosurfaces can be created for total gamma-ray and neutron counts or for gamma-ray energies associated with specific radionuclides.

Additionally, by flying near hard-to-reach surfaces, an sUAS can benefit from radiation's inverse distance-square intensity drop, significantly increasing its detection sensitivity to weak, buried, or shielded materials to generate detailed volumetric radiation maps. Having an unmanned system carry the LAMP system near radioactive sources also limits radiation exposure to the human operator.

To date, such real-time systems require two independent operators— one controlling the sUAS and another interpreting radiation readings on a 2D monitor [3], [5], [6]. The requirement for the two operators to manually synchronize mission-critical data may compromise real-time response to time-critical information. Furthermore, current systems are limited by a lack of stereoscopic depth cues on traditional 2D monitors when viewing 3D data.

Our system overcomes these limitations by allowing just

978-1-7281-7693-2/20/$31.00 ©2021 IEEE

a single operator to perform radiation mapping missions and view incoming data in its native, three-dimensional form. We employ Virtual Reality (VR) technology and semi-autonomous sUAS flight control to streamline operation, thereby enabling one person to simultaneously command the sUAS and monitor mapped radiation. Stereoscopic depth cues intrinsic to VR convey enhanced spatial understanding of 3D data [7], [8], [9], which is critical for remote sUAS control. Furthermore, the combination of remote sUAS control and VR interfaces has been shown to offer more intuitive and efficient flight planning experience [10] for operators without in-depth knowledge of sUAS systems [11]. Our work integrating data visualization with sUAS control in a VR interface enables the operator to make radiologically informed decisions without relying on a separate pilot or interpreter. It will also provide the basis to operate sUASs remotely and out of line-of-sight, providing more effective and safer deployments.

In this work, we present a system that integrates real-time 3D radiation mapping with semi-autonomous sUAS control. We use widely available commercial VR and drone navigation systems to enable a sole operator to safely conduct radiation detection missions as shown in Figure 1. Section II covers the hardware of our three main components— the sUAS, the attached LAMP system, and the VR interface. Section III covers the software needs of our system— first, the communication implementation between the main components, and then the software of each component individually. Finally, Section IV details the VR interface: how contextual environment data is visualized, how the operator controls the sUAS for mapping purposes, and how the measured radiation intensity data is visualized.

II. System Hardware

Our system consists of a semi-autonomous sUAS carrying a LAMP sensor (Figure 2) that communicates with a remote VR interface as shown in Figure 3. Specifically, an sUAS is safer to fly in urban environments over a fixed-winged aircraft due to its ability to fly slowly or hover in place. To control the sUAS, the operator sends commands via the VR interface, which also receives and displays radiation maps constructed by the LAMP instrument. Our system relies on WiFi to communicate between the sUAS and the interface, but we expect that future systems will utilize cellular networks instead to increase operational range. A summary of the specifications for the sUAS, LAMP, and WiFi connectivity can be found in Table I.

A. sUAS Hardware

To replicate previous works that used an sUAS-mounted LAMP [3], we chose the DJI Matrice 600 (M600) hexacopter as the system's sUAS for its semi-autonomous capabilities, flight time, and 6-kg payload capacity. An M600 with an attached LAMP system is shown in Figure 2. Previous works that used the M600 had one of its operators fly it manually using a remote controller. This required constant and real-time human input to ensure safe flight around the region being mapped. Instead, our system is built to use the M600's semi-autonomous flight mode to remove the need for a full-time pilot. The M600 is able to receive and autonomously execute flight commands such as take-off; fly to a location specified by a latitude, longitude, and altitude; and land back at the take-off location. These capabilities can abstract away significant piloting work from the operator.

Fig. 2. Our sUAS is a DJI Matrice M600 that carries a LAMP sensor. In the image, the LAMP system can be seen underneath the sUAS and includes a LiDAR puck. The attached white box contains the radiation detection or imaging instrument.

The flight time of the sUAS when it is fully loaded with 6-kg of payload is roughly 16 minutes. This is sufficient for mapping small buildings as shown in Figure 1 and larger structures and areas based on typical speeds ranging from 1 m/s to 5 m/s. The final reason for using the M600 is that, upon takeoff, it retracts its landing gear, providing the bottom-mounted ranging sensors with unobstructed lateral and downward views.

For accurate positioning during flight and for visualization of the sUAS in VR, we chose the DJI Real Time Kinematic GPS (RTK-GPS) module which provides centimeter-level 3D positioning data. The RTK-GPS module comprises a ground station and dual antennae on-board the sUAS. Its localization aids the aircraft in following the set waypoint path

TABLE I
Operational characteristics of sUAS, LAMP, and WiFi connectivity.

System Design Parameters	
WiFi (2.4 GHz) Range Outdoors (Theoretical)	91.44 m
WiFi (2.4 GHz) Range Outdoors (Practical)	approx. 20 m
WiFi (2.4) Range With Building Interference	approx. 15 m
4G / 5G Cellular Network Range Outdoors	Anywhere with 4G / 5G
M600 Payload Limit	6 kg
M600 Flying Time with Max Payload (6 kg)	approx. 15 min
NG-LAMP Weight	4.2 kg
M600 + LAMP Operational Flight Speed	1–5 m/s
NG-LAMP Field of View	4π steradians
NG-LAMP CLLBC Detector Volume	131 cm^3
NG-LAMP Gamma-ray Energy Resolution	3.6% at 662 keV
NG-LAMP Dimensions	30 cm x 16 cm x 20 cm
NG-LAMP Battery Lifetime	approx. 60 min
LIDAR Max Range	80m
LIDAR Horizontal Field of View	360°
LIDAR Vertical Field of View	$\pm$ 30°

autonomously and prevents the sUAS from drifting when it is hovering in-place or landing. As our sUAS frequently flies closer than two meters to buildings, this robust localization is integral to avoiding collision even when buffeted by strong winds. This accurate positioning improves both sUAS control and visualization in VR.

B. LAMP Hardware

The sUAS carries a LAMP radiation detection instrument which maps radiation sources and their contextual environment. A wide range of radiation detection and imaging instruments can be attached to the LAMP producing isosurfaces showing the localization and intensity of radiation sources. LAMP has been integrated with simple $LaBr_3$ detectors, CLLBC ($Cs_2LiLa(Br,Cl)_6$:Ce) detector arrays, and arrays of coplanar-grid CdZnTe detectors implemented as a broad-energy and omni-directional gamma-ray imaging instrument. In particular, for the figures in this paper, a LAMP system fitted with CLLBC detectors has been used for gamma-ray and neutron detection and mapping, utilizing the high sensitivity and energy resolution for gamma rays and high sensitivity for thermal neutrons. This so-called Neutron-Gamma LAMP (NG-LAMP) consists of 4 CLLBC detectors, each 1"x1"x2" in dimension and arranged as a 2x2 array forming approximately a 2"x2"x2" cube. LAMP is also equipped with a Velodyne VLP-16 Light Detection and Ranging (LiDAR) puck and an inertial measurement unit (IMU) whose data are combined by running a simultaneous localization and mapping (SLAM) algorithm [12] to generate a surface pointcloud. The LAMP further contains an Intel NUC single board computer running the localization, sensor fusion, and meshing algorithms to periodically publish the radiation and environment mesh data. While the NUC computer is part of LAMP for radiation mapping purposes, we also use it to communicate with the sUAS, avoiding the need for an additional on-board computer. The NUC is connected to the sUAS over a USB interface and is connected to the computer running the VR interface via a WiFi connection to relay mapped radiation, GPS coordinates, and waypoint commands during flight as shown in Figure 3. For more information about the specifications and operation of the LAMP system, please refer to previous works such as [2], [3]

C. VR Hardware

The user interacts with the virtual reality interface using the Oculus Rift S system which consists of a head mounted display and hand-held controllers as shown in Figure 4. The Rift S is widely used and is a commercially affordable VR system, making it an ideal platform for widespread impact. The hand-held controllers allow the operator to interrogate the VR visualizations as well as direct the sUAS flight plan. Displaying the radiological and flight information, the headset renders depth cues beyond the traditional display's simulation (i.e. perspective, shading, occlusion, and atmospheric hue-shift effects) by adding stereopsis and parallax. By containing an independent display for each eye, graphics are displayed with parallax disparity for the baseline between the eyes, recreating

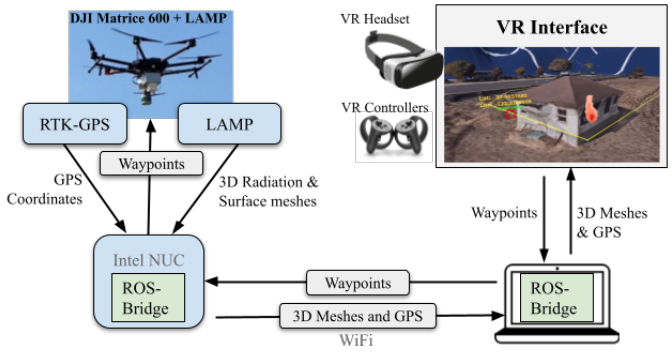

Fig. 3. Workflow of deploying a radiation-mapping mission between an sUAS (left) and the VR interface (right). Waypoints are placed on the 3D map in VR and transmitted over WiFi as geolocated flight targets for the sUAS to reach semi-autonomously. Operators can view the real-time LAMP radiation and surface reconstruction from the sUAS in VR.

stereoscopic depth cues. The operator of our VR interface utilizes the depth perception to perceive the 3D location of the sUAS and waypoints in relation to the static satellite imagery map. And when sensor data is visualized in VR, the depth perception allows the operator to observe mapped radiation and surfaces in their native 3D geometry. In addition to providing stereoscopic depth perception, the headset also continuously tracks its own pose with 6 degrees of freedom allowing it to simulate head movement-based parallax depth cues. The scene is rendered to match the user's head's pose as if the user is "inside" the scene and enables naturalistic viewpoint control. For example when the user looks down at the ground, the scene shows what is directly below the user. The operator can use this feature to look around the map and behind buildings as the sUAS flies.

The Rift S hand-tracking controllers afford a variety of interaction schemes with the VR environment. Each of the two controllers has three buttons and a joystick actuated with the users' thumbs, as well as grasp sensors actuated with the user's index and middle fingers. These input methods can be used to interact with the scene as illustrated in the interface we will describe in subsection IV-C. Furthermore like the headset, the pose of the hand-held controllers is continuously tracked with 6 degrees of freedom. In turn, the controllers are visualized in the scene and mimic the user's hand movements in real life. Within this VR world, they serve as virtual hands or pointers so that the user can interact with the scene.

Wired VR headsets, like the Rift S, typically require a VR-compatible computer— a machine with the prerequisite graphical processing power to render the 3D scene in real-time. Our system was run by a machine with a NVIDIA GTX 1060 graphics card, 8 GB of RAM, and a DisplayPort video output. We typically used our VR system outdoors, but the tracking quality would suffer in direct sunlight and solar radiation would deteriorate the VR displays. To mitigate these issues, the VR operator worked in a shaded outdoor location.

III. System Software

Using these hardware platforms, we developed software to combine the LAMP output data, sUAS control, and VR

Fig. 4. A user can equip a VR headset and control the sUAS with VR controllers.

subsystems. As a whole, the system software has four main responsibilities: providing subsystem communication channels, executing LAMP mapping algorithms, controlling the sUAS, and interfacing with the operator through VR.

A. Communications Software

We chose the Robot Operating System (ROS) [13] to provide all necessary communication between the three major subsystems: the LAMP, sUAS, and VR interface. It provides the necessary flexibility and modularity for the two-way web socket communication across multiple platforms over WiFi and enjoys broad community support and usage. Specifically, it enables the transmission of operator-selected waypoints and the GPS coordinates of the sUAS between the VR interface and the sUAS, and the radiation maps between the LAMP instrument and the VR interface.

B. LAMP Software

Alongside the hardware summarized in Sec. II-B, LAMP contains an integrated computer that processes the data generated in near real-time to create a 3D model of the environment and associates the observed radiation detector events with the observed surroundings. The LiDAR and IMU data generated by LAMP are processed on-board using SLAM. SLAM outputs a point cloud and instantaneous LAMP system poses within that point cloud. Using the pose of the radiation detectors, a probabilistic model is formulated to describe the probability that each observed radiation event is emitted from each pixel of the observed 3D model. Depending on the specific LAMP implementation, radiation reconstruction algorithms are being used taking into account the detection or imaging system response matrix. For example, a proximity or coded aperture modes can be selected in combination with List-Mode Maximum Likelihood Expectation Maximization or with Point Source Localization [14], [15].

In order to enable a reliable data transfer from the LAMP system to the VR interface, the point-clouds and reconstructed radiation data are converted into 3D meshes which are then transmitted via WiFi. The radiation reconstruction, data fusion and conversion from the point clouds to the meshes is done by the NUC computer of the LAMP on board the sUAS. To further reduce the burden on the data transfer, only the last reconstructed portions of the meshes are transmitted for visualization. In this way, a data rate of less than 1 MB/s can be achieved which can be sustained by the WiFi.

C. sUAS Software

Typically the DJI Matrice is equipped with an additional DJI-made on-board computer that controls the sUAS via the DJI Software Development Kit (SDK). Instead of using this additional computer, to reduce complexity, our system utilizes the LAMP's computer itself to run the DJI Onboard SDK v3.8.1 [16] and convert between the VR interface's commands and the sUAS's control logic. The DJI SDK publishes ROS topics detailing the spatial and state information about the sUAS such as /rtk_position, /battery_state, /attitude, etc., that the VR interface subscribes to for real-time visual feedback to the operator in VR. The DJI SDK allows for ROS service calls to control the sUAS such as take/relinquish authority, takeoff/land, pause/resume flight, upload waypoint mission, etc., that are used by the VR interface to control the sUAS as per operator commands.

D. VR Interface Software

The VR interface receives data from the LAMP, and after parsing it, converts the radiation and LiDAR data into meshes that are then overlaid on a satellite-imaged 3D map. It also receives the sUAS's GPS coordinates which are used to position the sUAS model in relation to the satellite map. In addition to visualization, the VR interface is used by the users for placing waypoints for the sUAS to follow. Waypoints placed in the interface are converted to real-world coordinates and then converted into ROS service calls that leverage the DJI SDK to control the sUAS.

The engine that supports the VR interface must provide high-fidelity graphics efficiently, so any real-world observations made by the sUAS are quickly and accurately reflected within the interface. This makes game engines a great choice. The VR application is therefore built on Unity [17], an industry-standard simulation development platform that provides tools to create a high quality interface for the VR user and to render meshes in real-time efficiently. It also supports two-way web socket connections and data streaming and pairs well with ROS. Additionally, our interface uses the Virtual Reality Toolkit (VRTK) [18], a package that extends Unity's support to VR applications and to work with many popular VR headsets, including ours.

IV. Virtual Reality Interface

A. Virtual Reality User Interface Overview

Radiation mapping via an sUAS is typically conducted using at least two operators with independent interfaces to perform

the task. One operator pilots the sUAS via a hand-held remote controller and the other monitors radiation reconstructions on a 2D display. The two operators communicate with each other about the sUAS's flight path in order to ensure quality mapping is achieved. This manual synchronization of mission-critical data may compromise real-time response to time-critical information. In addition, the monitoring operator is limited to viewing inherently 3D data on a 2D display, which can limit their understanding of mapping results.

Virtual Reality headsets employ stereoscopic displays to induce depth perception for the viewer, thus making rendered 3D geometry more realistic than on 2D displays. Such an interface alleviates the cognitive demands posed by the current system in three ways. First, a VR interface provides the operator with depth perception which enhances the viewing of 3D data compared to viewing it on a 2D display. Second, the VR interface allows us to combine the roles of the sUAS operator and radiation monitor into a unified interface handled by a sole operator, which removes the need for communication. The graphical control mechanisms for directing the sUAS's flight are situated in the same view as the radiation readings in order to allow the single operator to perform both monitoring and piloting tasks. Finally, we take advantage of the three-dimensionality of the VR interface to provide a 3D waypoint-based flight system to command the aerial vehicle during mapping missions. The user-defined waypoint-placement system utilizes our sUAS's semi-autonomous capabilities to reduce the operator's cognitive load necessary to guide the sUAS. This point-and-click system simplifies the workflow of mapping missions, enabling operators to focus on radiation mapping instead of vehicle maneuvering. The VR interface is an intuitive choice for interacting with 3D data, and for utilizing a waypoint system for semi-autonomous flight. In the remainder of Section IV we describe the visualization of the contextual environment and the sensor data, how the user interacts with the visualizations, and commands the sUAS via the waypoint-placement system.

When wearing a VR headset, the operator's view is limited to the VR display, thus we aim to mimic relevant parts of the real world within the VR environment. The VR environment is initially composed of a sUAS model and a baseline 3D view of the sUAS's surroundings derived from prior satellite imagery, as shown in Figure 5. The 3D satellite imagery remains static throughout the sUAS operation, but is augmented in real-time with radiation and contextual data as they are collected by the on-board LAMP system. In the virtual environment, the operator can orient themselves by panning, rotating, and zooming the map. The operator can then command the sUAS to traverse specific geo-locations (waypoints) in the 3D environment. As the sUAS is launched and starts flying, the visualized sUAS model is constantly updated to reflect the GPS location of the physical sUAS. Concurrently, radiation and environment data received from the LAMP is overlaid on the environment baseline and augmented as the sUAS mission continues. The visualized radiation overlay, environment overlay, satellite imagery, waypoints, and sUAS all scale together to always provide an accurate representation of the real world to the operator. Radiation from the environment is visualized in the interface as a colorized 3D mesh depicting varying radiation intensity levels which can reflect total energy counts or radioisotope-specific counts. The environment mesh derived from the on-board LiDAR is seen as a gray overlay. Informative visuals such as sUAS battery levels and GPS signal strength are displayed. There are also menus where the user can toggle sensor data visualizations on and off. This real-time feedback of the sUAS's location and the data it has collected enhances the operator's ability to precisely assess the current situation and direct the mapping mission accordingly.

Fig. 5. Our VR interface consists of a baseline 3D mesh of the real world environment to orient the user in the virtual environment. The baseline mesh can be scaled or translated with arm gestures, allowing the user to navigate it while remaining stationary in the real world. Parked vehicles in this mesh may be used as a scale reference.

B. Environment Data Visualization

Upon starting the VR application, the operator's view into the scene includes the sUAS and its surroundings, which is a baseline representation of the real world as shown in Figure 5. This baseline representation is required to provide the operator a sense of scale and orientation. To establish this baseline, the operator is shown a 3D satellite-imaged mesh of the sUAS's environment as shown in Figure 5. This mesh is obtained from Google Earth and currently has to be pre-loaded for an area of interest, but there are future plans to integrate reconstructed aerial colorized 3D maps to provide real time visualization of this background mesh. This background map is strictly to provide the user a baseline of the sUAS's environment. A surface mesh of the environment, which is generated from LiDAR data, is also overlaid in real-time during the flight for a more holistic view of the current environment. Additionally, we display sUAS diagnostics, such as battery levels and GPS signal strength, in real time. The LiDAR environment data and sUAS diagnostics ultimately help provide the user with important information required to control the sUAS.

C. VR User Controls

As virtual reality interfaces provide an egocentric view for the operator, the operator must navigate within the virtual world in order to reach and interact with the 3D content. Additionally, viewing the content from different perspectives

requires the user to move and turn within the virtual world. In our interface, the user's main interaction is selecting geo-located waypoints at specific locations on the map for the sUAS to fly to. As such, the user must be able to reach all areas of the virtual world using their VR hand controllers in order to place waypoints. We support this requirement by allowing the operator to laterally move and rotate the map in order to reach all locations. Navigating the map also allows the operator to view the 3D environment and incoming data from any perspective so they can inspect the quality of the 3D radiation reconstructions and the sUAS's flight path. We provide the user a number of ways to move the virtual world so they may reach and inspect all relevant locations.

The operator interacts with the virtual environment using the two Oculus handheld controllers, which appear as VR hands in the interface. The operator can orient the virtual map by scaling, rotating, or translating it using these controllers. These orienting actions transform the visualized radiation reconstruction overlay, surface meshes, satellite imagery, and sUAS consistently to provide the operator an accurate real world representation. For instance, the operator can scale the map down or up by holding down the controllers' shoulder buttons and moving their arms together or apart, respectively. These gestures can intuitively bring different parts of the map in focus for the user without needing them to physically walk around the tabletop map.

To allow the operator control over data visualization, the sensor menu provides on/off toggles for visualizing data from the on-board sensors including the LiDAR and LAMP as shown in Figure 6. The user can cycle through all the sensors and customize the interface to reduce clutter and better focus on specific data. In particular, the interface can display a specific relative intensity level for user-defined energy ranges as measured in the gamma-ray spectrometer or neutron intensities when gamma-ray and neutron-sensitive detectors such as CLLBC are being used in combination with LAMP. For the purposes of this paper, we visualize only the gamma radiation as a proof of concept.

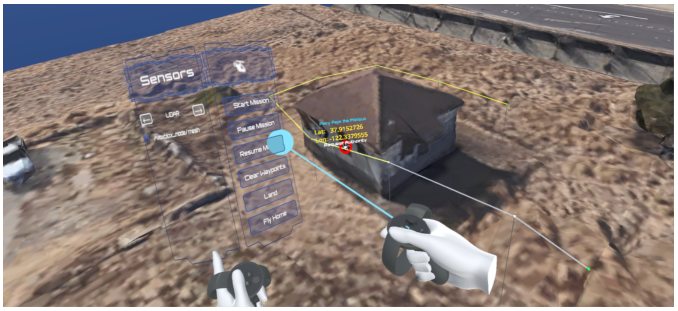

Fig. 6. Our VR interface displays a textured 3D view of the environment derived from prior satellite imagery. The operator sets waypoints through the VR interface to mark important flight path geo-locations. The sUAS (red) follows the flight path (yellow) around the building, detecting and streaming radiation and environment reconstruction data back to the interface as a colorized 3D mesh (not shown here). The operator uses their virtual hands to select from the left-controller's sensors and flight-controls menus via the cyan pointer to control sensor data visualizations and sUAS operation, respectively.

The flight-controls menu allows the operator to issue commands to an sUAS during a waypoint mission by pressing virtual buttons as shown in Figure 6. The operator can start, pause, resume, reset, and end missions using these commands. These missions are an ordered sequence of user-defined waypoints for the sUAS to follow, one after another. Mission waypoints can be placed by the user, as we detail in subsection D.

D. Waypoint-Placement System

Traditional sUAS piloting requires constant real time input of an operator and imposes line-of-sight restrictions on the sUAS to ensure informed control. Furthermore, areas with high interference levels can cause lag and, in the worst case, total loss of communication between the remote control and the sUAS, which is especially dangerous when the sUAS relies on constant, real-time input. Additionally, popular alternative control schemes such as first person view controllers tether the operator awareness to the sUAS and its immediate surroundings. The operator cannot issue commands to the sUAS and then divert their attention to other parts of the scene.

On the other hand, waypoint missions provide a better system to conduct missions efficiently and safely. Waypoints can be prepared before a mission begins, and an operator can study different parts of the scene as the sUAS semi-autonomously follows the waypoints while transmitting radiation readings. Operators can therefore study radiation readings across the whole scene as they are collected and adjust the flight path accordingly. Furthermore, under semi-autonomous control the sUAS can better navigate areas with high-interference by accepting a pre-defined flight path and following it without requiring constant, live input.

Moreover, our waypoint system allows the operator to intuitively control the semi-autonomous sUAS without needing extensive pilot training. To create a waypoint, the operator simply moves their hand to a target location and pushes a button to mark that location with a sphere. As more waypoints are added, these target locations are connected, resulting in a fight trajectory as seen in Figure 1 and Figure 7.

The operator can edit each waypoint as needed, and initiate the sUAS mission when satisfied with the flight path. The VR interface converts the in-app waypoint locations to real-world GPS coordinates. Subsequently, the sUAS executes the flight path, flying to each waypoint in the set order at a set velocity. The sUAS typically flies at about 1 meter per second, but the velocity is adjustable. The operator can edit the future waypoints during the sUAS flight to update the flight path upon analyzing the live-streamed radiation as in Figure 7.

With waypoint missions, the operator only needs to select important targets for the sUAS, while the flight path is automatically interpolated between them. Our system abstracts away flight controls and stabilization, reducing the operator's cognitive load and need for piloting expertise.

E. Sensor Data Visualization

After a waypoint mission is finalized and uploaded, the sUAS begins traversing its path of geo-locations. As the sUAS flies in the real world, on-board sensors gather and stream data back to the interface.

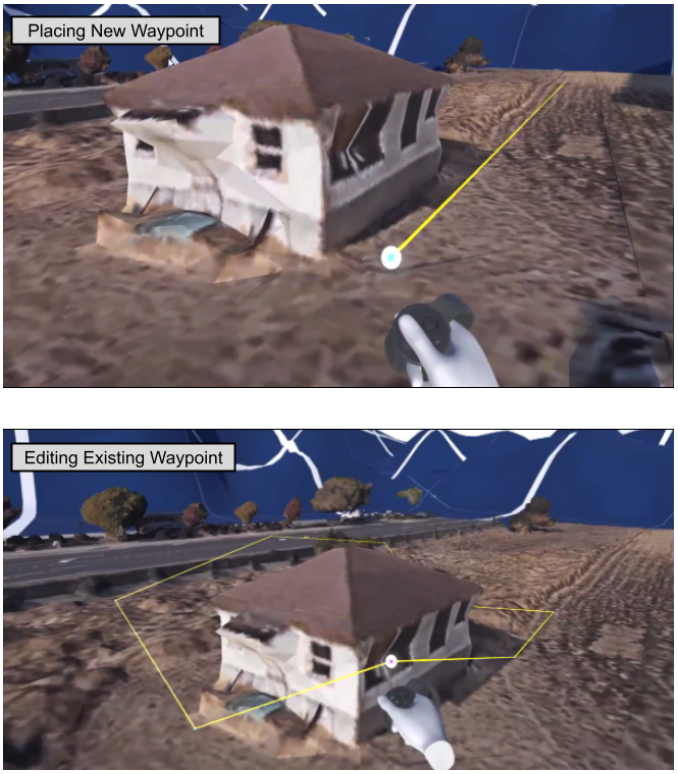

Fig. 7. The user can define a waypoint mission by placing waypoints in the virtual environment using the right-hand controller. After the waypoints are sent from the VR world to the sUAS, the sUAS will follow each waypoint in order while constantly relaying radiation and environment reconstruction data back to the interface as it flies. The user can also edit a waypoint before or during a mission with the right-hand controller. The waypoint being edited is colored in purple in the above image. The updated waypoint is instantly sent to the sUAS to automatically adjust the current flight path to include the new waypoint instead of the old one.

LiDAR-generated surface data is received as a mesh, and then overlaid on the pre-loaded, static satellite map. While the satellite map may have contained old, historical data, this 3D surface mesh provides a highly accurate, real-time reconstruction of the real world, allowing the user to see any obstacles or structures not included in the baseline map. Since the sUAS lacks obstacle avoidance, the user relies on the satellite map and surface mesh to ensure the safety of the sUAS. However, we anticipate integrating automatic obstacle avoidance in the future. This updated knowledge about the environment allows the user to make decisions in real-time about where to place waypoints. The LiDAR-surface mesh can be toggled on or off by the user with the sensor UI on the left hand.

Radiation from the environment is visualized in the interface as colorized 3D meshes as shown in Figure 8. While existing systems display radiation data as a top-down view on a 2D display, we are visualizing 3D data in 3D space. This provides a more meaningful understanding of the environment, as the user can accurately pinpoint a source to its 3 real-world spatial dimensions.

The LAMP sensor streams 6 separate radiation isosurface meshes, each corresponding to a linearly increasing level of radiation intensity. A color scale from light to dark red depicts these six isosurfaces. (Figure 8). This color coding adds visual cues for the user to easily distinguish between strong and weak measurements, and visually locate a radioactive source. This figure illustrates measurements performed with the so-called NG-LAMP. List-mode maximum-likelihood expectation-maximization is being performed for the image reconstruction. A 1.7-mCi Cs-137 source within 2 cm of lead shielding was placed behind one of the windows in the building. For the shown reconstruction, an energy window was placed around the 662-keV photopeak associated with Cs-137. Using the sensor UI on the left hand, each of the 6 meshes can be toggled on or off to focus on specific levels of interest. In Figure 8 we visualize the top 5 (of 6) radiation meshes, corresponding to the top 83 percent of radiation intensities detected.

The radiation meshes are visualized on top of the real-world environment reconstruction, giving the operator an immersive understanding of the world. The merged visualization gives the user enhanced vision, overlaying both the typical environment and radiation intensities at every point in 3D space.

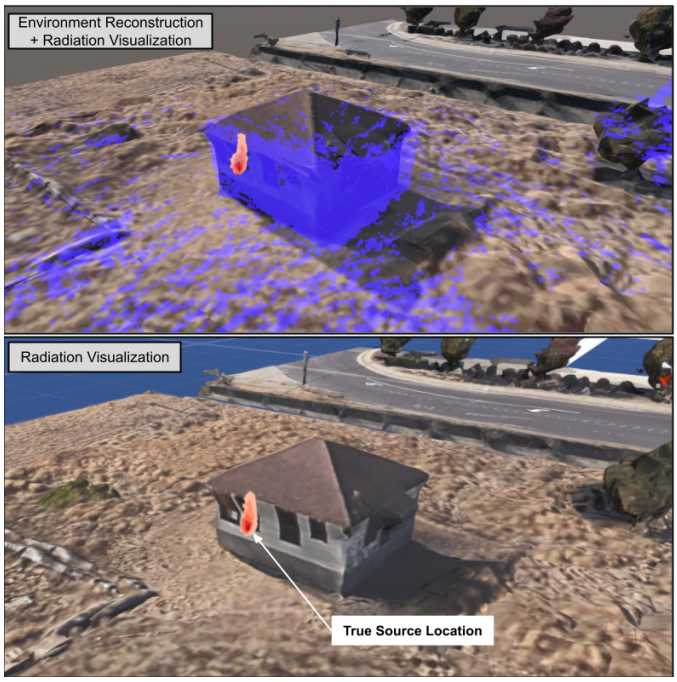

Fig. 8. Our system streams radiation and environment reconstruction data back to the VR interface, shown here, as colorized 3D meshes. The environment reconstruction (top, in purple) is generated by the LAMP's LiDAR and is used for the radiation reconstruction. We overlay the environment reconstruction on the baseline map to provide an accurate, real-time view of the sUAS's surroundings to the operator. The radiation-only visualization (bottom) shows reconstructed intensities of 662 keV reflecting measurements of the gamma-ray energies with the CLLBC-based NG-LAMP. Higher gamma-ray intensities are denoted by darker shades of red. Note we display only the 5 (of 6) most intense gamma-ray isosurfaces for visualization purposes. The operator can therefore intuitively localize the source to the darkest part of the mesh. For reference, the square building has a side length of about 8 meters.

Our system provides the operator the flexibility to rapidly adapt the flight path in response to this received data. With an enhanced understanding of the situation, the operator can place new waypoints to localize a radiation source, determine

the range of a radiation leak, or to meet any other mission specific needs.

V. Future Work

This work presents several opportunities for further novel engineering. This includes diversifying the types of radiation sensors, running missions with multiple sUASs, extending semi-autonomous optimization, and expanding the reconstruction visualization to more users.

A. Diversifying radiation sensing

While we demonstrated the new control, mapping, and visualization capabilities with the CLLBC detectors as gamma-ray spectrometers, the system can handle other gamma-ray detection and imaging systems. Integrating other sensors could provide a wide range of radio-isotopic maps with high specificity and accuracy. This opens new possibilities for how the diverse radio-isotopic maps should be super-imposed for informativeness. Different sensors could also furnish neutron maps relevant in the detection and localization of so-called special nuclear materials which emit gamma rays and neutrons.

B. Scaling to multiple robots

In parallel to diversifying the sensing hardware, there is an opportunity for diversifying the flight hardware and building up a heterogeneous sensing swarm. The system presented has been made to work with DJI-based sUASs but can be simply expanded to work with different sUAS designs. With this added flexibility, the system can expand to operate multiple sUASs, with possibly varying designs or heterogeneous sensor capabilities simultaneously, thereby expediting a pilot's ability to map widespread terrain. Managing the data-flow from a swarm of sUASs and synchronizing their reconstructions will require some kind of centralized (server-based) architecture before communicating with the VR interface.

C. Extending semi-autonomy

The semi-autonomy already used to reduce operator piloting overhead could be expanded to automatically suggest waypoints of interest. Ultimately, the operator would only need to approve a plan from a selection of generated flight paths rather than lay it out by hand. Combining the operator's mission understanding and intuition with optimal path planning for shortest flights would create more efficient deployments. Such algorithms could aim at minimizing the time to detect a source or to map specific radiation and dose-rate levels in complex 3D environments.

D. Expanding to Teams of Operators

One other area of interest is the visualization itself. Currently, only a single operator can view the map, including the radiation meshes on it. One potential improvement to this setup is allowing multiple interfaces to attach to a single system, letting multiple users control the sUAS or view the meshes. The system could also let more people into the same virtual "room". That way, although a single operator controls the sUAS, multiple users can watch the map as the mesh is generated. Additionally, the system could incorporate AR visualizations as well as the VR interface. In order to execute manned missions, a remotely operating system, controlled for example by the developed VR interface could map out the radiation just ahead of personnel on the ground. Once the personnel is equipped with augmented reality glasses they could see the surrounding radiation fields and navigate while mitigating their exposure to the radiation. This can be done synchronously with the remotely operating system performing the mapping while the ground personnel is executing its mission, or asynchronously with the remotely operating system completing the mapping mission first before the ground personnel executes its mission. Finally, the current concept which utilizes WiFi-based control and data transfer could be extended to cellular networks to enable longer ranges and truly remote operations.

VI. Conclusion

We introduced a novel immersive system that enables a single operator to simultaneously map radiation, visualize that map in 3D, and then followup to direct the sUAS to gather more scans. Existing systems have separate mapping and control interfaces, therefore relying on two operators—one to fly the sUAS and the other to oversee the mapping operation. With our unified interface, a sole operator is able to do both tasks with enhanced spatial awareness and reduced burden for control. This streamlining required delegating the moment-to-moment flight control to the semi-autonomous sUAS and visualizing the radiation and environment data three dimensionally in the same interface as the controls. Our virtual reality interface shows a model of the sUAS in its environment and allows the operator to place geo-located flight goals, or waypoints, to navigate the sUAS in the real world. From take-off onward, the LAMP-equipped sUAS maps its environment and any located radiation, transmitting the visualization to the interface, enhancing the operator's understanding of the sUAS's position in real-time and the currently radiation-mapped areas. We have successfully demonstrated this new concept by utilizing a sUAS equipped with a Localization and Mapping Platform in combination with an array of CLLBC detectors at the UC Berkeley-managed Richmond Field Station. This combined mapping-and-control interface successfully flew a sUAS to map the 3D environment of a building and localize a shielded Cs-137 source within this building.

We believe that our system will help make radiation mapping missions safer, easier, and more efficient. Combining radiological visualization and semi-autonomous flight control all in one interface creates a closed-loop for scanning previously-unreached areas. The information density and interactive capacity of VR makes it a rich platform for converging technologies to empower users. This approach is poised to integrate even more human and machine intelligence towards even greater ends.

REFERENCES

[1] K. Vetter, R. Barnowski, J. W. Cates, A. Haefner, T. H. Joshi, R. Pavlovsky, and B. J. Quiter, "Advances in nuclear radiation sensing: Enabling 3-d gamma-ray vision," *Sensors 19(11) (2019) 2541*, Jun 2019.

[2] R. Pavlovsky, A. Haefner, T. Joshi, V. Negut, K. McManus, E. Suzuki, R. Barnowski, and K. Vetter, "3-d radiation mapping in real-time with the localization and mapping platform lamp from unmanned aerial systems and man-portable configurations," *arXiv preprint arXiv:1901.05038*, 2018.

[3] R. Pavlovsky, J. Cates, W. Vanderlip, T. Joshi, A. Haefner, E. Suzuki, R. Barnowski, V. Negut, A. Moran, K. Vetter *et al.*, "3d gamma-ray and neutron mapping in real-time with the localization and mapping platform from unmanned aerial systems and man-portable configurations," *arXiv preprint arXiv:1908.06114*, 2019.

[4] Y. Sato, S. Ozawa, Y. Terasaka, M. Kaburagi, Y. Tanifuji, K. Kawabata, H. N. Miyamura, R. Izumi, T. Suzuki, and T. Torii, "Remote radiation imaging system using a compact gamma-ray imager mounted on a multicopter drone," *Journal of Nuclear Science and Technology*, vol. 55, no. 1, pp. 90–96, 2018.

[5] D. Connor, P. G. Martin, and T. B. Scott, "Airborne radiation mapping: overview and application of current and future aerial systems," *International Journal of Remote Sensing*, vol. 37, no. 24, pp. 5953–5987, 2016. [Online]. Available: https://doi.org/10.1080/01431161.2016.1252474

[6] D. T. Connor, K. Wood, P. G. Martin, S. Goren, D. Megson-Smith, Y. Verbelen, I. Chyzhevskyi, S. Kirieiev, N. T. Smith, T. Richardson, and T. B. Scott, "Radiological mapping of post-disaster nuclear environments using fixed-wing unmanned aerial systems: A study from chornobyl," *Frontiers in Robotics and AI*, vol. 6, p. 149, 2020. [Online]. Available: https://www.frontiersin.org/article/10.3389/frobt.2019.00149

[7] A. Cardoso, G. F. Cyrino, J. C. Viana, M. J. Junior, P. A. Almeida, E. A. Lamounier, and G. F. Lima, "Use of virtual and augmented reality as tools for visualization of information: A systematic review," in *International Conference on Intelligent Human Systems Integration*. Springer, 2019, pp. 407–417.

[8] Y. Sato, Y. Terasaka, S. Ozawa, Y. Tanifuji, and T. Torii, "A 3d radiation image display on a simple virtual reality system created using a game development platform," *Journal of Instrumentation*, vol. 13, no. 08, p. T08011, 2018.

[9] J. T. Hansberger, S. Meacham, and V. Blakely, "Designing data & dashboard visualizations for future uav systems," in *Proceedings of the Human Factors and Ergonomics Society Annual Meeting*, vol. 62, no. 1. SAGE Publications Sage CA: Los Angeles, CA, 2018, pp. 177–181.

[10] J. R. Paterson, J. Han, T. Cheng, P. H. Laker, D. L. McPherson, J. Menke, and A. Y. Yang, "Improving usability, efficiency, and safety of uav path planning through a virtual reality interface," in *Symposium on Spatial User Interaction*, 2019, pp. 1–2.

[11] J. J. Roldán, E. Peña-Tapia, D. Garzón-Ramos, J. de León, M. Garzón, J. del Cerro, and A. Barrientos, "Multi-robot systems, virtual reality and ros: Developing a new generation of operator interfaces," in *Robot Operating System (ROS)*. Springer, 2019, pp. 29–64.

[12] W. Hess, D. Kohler, H. Rapp, and D. Andor, "Real-time loop closure in 2d lidar slam," in *2016 IEEE International Conference on Robotics and Automation (ICRA)*, 2016, pp. 1271–1278.

[13] Stanford Artificial Intelligence Laboratory et al., "Robotic operating system." [Online]. Available: https://www.ros.org

[14] R. Barnowski, A. Haefner, L. Mihailescu, and K. Vetter, "Scene data fusion: Real-time standoff volumetric gamma-ray imaging," *Nuclear Instruments and Methods in Physics Research Section A: Accelerators, Spectrometers, Detectors and Associated Equipment*, vol. 800, pp. 65–69, 2015. [Online]. Available: https://www.sciencedirect.com/science/article/pii/S016890021500950X

[15] D. Hellfeld *et al.*, "Gamma-ray point-source localization and sparse image reconstruction using poisson likelihood," *IEEE Transactions in Nuclear Sciences*, vol. 66, no. 9, pp. 2088–2099, Sept. 2019. [Online]. Available: https://ieeexplore.ieee.org/document/8768340

[16] DJI, "Dji onboard sdk." [Online]. Available: https://developer.dji.com/onboard-sdk/

[17] J. Jerald, P. Giokaris, D. Woodall, A. Hartbolt, A. Chandak, and S. Kuntz, "Developing virtual reality applications with unity," in *2014 IEEE Virtual Reality (VR)*. IEEE, Mar. 2014. [Online]. Available: https://doi.org/10.1109/vr.2014.6802117

[18] VRTK, "Virtual reality tool kit." [Online]. Available: https://vrtoolkit.readme.io/